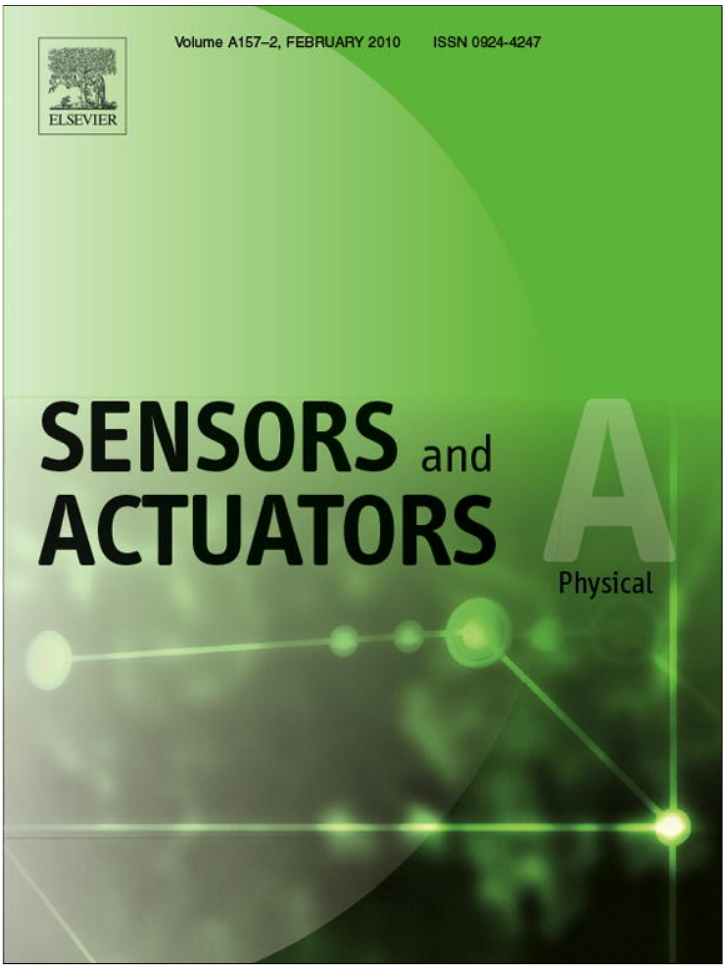

Sensors and Actuators A 157 (2010) 246–257

Contents lists available at ScienceDirect

Sensors and Actuators A: Physical

journal homepage: www.elsevier.com/locate/sna

Monolithic fabrication of ionic polymer–metal composite actuators capable of complex deformation

Zheng Chen, Xiaobo Tan*

Smart Microsystems Laboratory, Department of Electrical & Computer Engineering, Michigan State University, East Lansing, MI 48824, USA

ARTICLE INFO

Article history:
Received 6 August 2009
Received in revised form 29 October 2009
Accepted 24 November 2009
Available online 16 December 2009

Keywords:
Ionic polymer–metal composites
Biomimetic actuation
Complex deformation
Batch-fabrication
MEMS

ABSTRACT

Ionic polymer–metal composites (IPMCs) are soft actuation materials with promising applications in robotics and biomedical devices. However, traditional IPMC actuators can generate the bending motion only. In this paper, a lithography-based approach is presented for monolithic, batch-fabrication of IPMC actuators that are capable of complex deformation. Such an actuator consists of multiple, individually controlled IPMC regions that are mechanically coupled through compliant, passive regions. Two novel techniques have been introduced to overcome challenges in fabrication of patterned IPMCs: (1) selectively thinning down Nafion using reactive ion etch, to make the passive areas thin and compliant, and (2) modulating the stiffness and swellability of Nafion with ion-exchange. Ion-exchanged Nafion shows almost 300% increase in stiffness, and over 94% reduction in swellability in water and acetone, which facilitates lithography and other critical fabrication steps. Prototypes of artificial pectoral fins have been fabricated with the proposed method, and sophisticated deformation modes, including bending, twisting, and cupping, have been demonstrated. For example, a peak-to-peak twisting angle of 16° is achieved under 3 V, 0.3 Hz actuation voltages, showing the promise of the fabricated device in robotic fish applications.

1. Introduction

Ionic polymer–metal composites (IPMCs) [1,2] are soft, resilient polymeric materials that can generate large deformation under a low actuation voltage (several volts). An IPMC sample typically consists of a thin ion-exchange membrane (e.g., Nafion), chemically plated on both surfaces with a noble metal as electrode [3]. When a voltage is applied across an IPMC, transport of cations and solvent molecules within the membrane, and the associated electrostatic interactions lead to bending motions, and hence the actuation effect. Since IPMCs work well both in air and under water, they are very attractive for many applications, such as biomedical devices and biomimetic robots [4–11].

Fabrication techniques for IPMCs have been developed by several research groups [1,12] based on commercially available ion-exchange membranes such as Nafion. A casting process has been developed to fabricate thin (down to 20 μm) IPMC actuators [6,13]. Kim and Shahinpoor fabricated thick IPMCs (up to 2 mm) by baking the mixture of Nafion powder and solvent in a mold [14]. Plasma treatment was introduced to roughen the Nafion surface and improve the actuation performance of IPMC [15]. Chung et al. applied silver nano-powder in fabrication of IPMC to improve the adhesion between metal and polymer [16]. Akle et al. developed direct assembly plating method to make electrodes and produced high-strain IPMC [17].

IPMC produced with the aforementioned fabrication methods can only generate bending motions. However, actuators capable of complex deformation are highly desirable in many applications, such as contour control of space inflatable structures [18], biomimetic robots [19,20], and tunable mirror membranes [21]. One inspiring example in biology is the pectoral fin of a sunfish, which produces sophisticated conformational changes to achieve efficient locomotion and maneuvering [22]. The complex shape change is enabled by multiple muscle-controlled, relatively rigid fin rays that are connected via collagenous membrane. Several groups have assembled discrete components to make such multiple degree-of-freedom (MDOF) actuators [19,20]. However, the performance of assembled actuators was limited by complex structure design, friction among the components, and low energy efficiency in force transmission. While MDOF IPMC actuators can be obtained by manually removing the metal electrode of IPMC in certain areas [23], this approach is time-consuming and not amenable to miniaturization and batch-fabrication. Monolithic fabrication of MDOF IPMC actuators with a simple structure will be essential to improve the performance, reduce the cost, and enable mass production.

Efforts have been made in fabrication of patterned IPMCs by Jeon et al. [24–26], where they combined electroplating with electroless plating to selectively grow platinum electrodes on a Nafion film. In their work, however, tapes were used as masks to

* Corresponding author. Tel.: +1 517 4325671; fax: +1 517 3531980.
E-mail addresses: zc7u@virginia.edu (Z. Chen), xbtan@msu.edu (X. Tan).

0924-4247/$ – see front matter © 2009 Elsevier B.V. All rights reserved.
doi:10.1016/j.sna.2009.11.024

achieve patterning, which would not be conducive to microfabrication or batch-fabrication. Lithography-based microfabrication of IPMC has also been pursued by several groups [27,28,24], where metal layers are deposited directly on Nafion to form electrodes. Without the critical ion-exchange and electroless plating processes, IPMCs fabricated this way typically are not highly active, and the metal electrodes tend to peel off under large deformation because of the poor metal–polymer bonding. Feng and Chen developed microfabrication-based IPMCs with arbitrarily defined shapes, where the ion-exchange and electroless plating steps were also incorporated [29]. However, the actuators fabricated with this approach have a single degree of freedom and can perform bending only.

The contribution of this paper is a new process flow for lithography-based, monolithic fabrication of highly active, MDOF IPMC actuators. Inspired by the structure of the sunfish pectoral fin, we propose to achieve sophisticated three-dimension (3-D) deformation by creating multiple IPMC regions that are mechanically coupled through compliant, passive membrane. Both the IPMCs and the passive regions are to be formed from a same Nafion film. There are two major challenges in fabricating such actuators. First, the passive areas can substantially constrain the motion of the active areas. An effective, precise approach is needed for tailoring the stiffness of the passive areas. Second, Nafion films are highly swellable in a solvent. Large volume change results in poor adhesion of photoresist to Nafion and creates problems in photolithography and other fabrication steps. To overcome these challenges, two novel fabrication techniques have been introduced: (1) selectively thinning down Nafion with plasma etch, to make the passive areas thin and compliant; (2) impregnating Nafion film with platinum ions, which significantly reduces the film swellability and allows subsequent lithography and other steps.

The developed fabrication process involves plasma etching, ion-exchange, lithography, physical vapor deposition (PVD), and electroless plating steps. Reactive ion etching (RIE) with oxygen and argon plasmas is used to selectively thin down the passive area of Nafion membrane with a patterned aluminum mask. An etch recipe has been developed to achieve a high etching rate of 0.58 μm/min without damaging the film. In IPMC fabrication, an ion-exchange step is usually performed immediately before electrode plating. However, we have found that impregnating Nafion with platinum ions through ion-exchange can also increase its stiffness by two to three times, and reduce its swellability in water and in acetone by over 94%. This has proven critical in successful photolithography-based patterning in that it ensures good adhesion of photoresist to the Nafion film. A positive photoresist, AZ9260, is used in photolithography to create thick patterns which are used as the mask in the electroless plating process to selectively grow platinum electrodes in IPMC regions. After IPMC is formed, we treat the sample with hydrochloride acid (HCl) to undo the effect of the stiffening process, which softens the passive areas and enhances the actuation performance.

As a demonstration, we have applied the proposed method and fabricated artificial pectoral fins, each with three IPMC regions. A characterization system consisting of a CCD camera and image processing software has been set up to quantify the deformations generated by the fabricated samples. We have verified that, by controlling the phase differences between the voltage signals applied to the IPMC regions, each artificial fin can produce sophisticated deformation modes, including bending, twisting, and cupping. For example, a twisting angle of 16° peak-to-peak can be achieved with actuation voltages of 3 V at 0.3 Hz, when the top and bottom IPMCs lead the middle IPMC in phase by ±90°. We have investigated the impact of the thickness of passive area, and verified that the thinner the passive region, the larger the deformations. This has thus provided supporting evidence for our approach of modulating mechanical stiffness through plasma etching. We have further performed preliminary studies of the fabricated fins in underwater operation using a Digital Particle Image Velocimetry (DPIV) system. Interesting flow patterns are observed when the fin is actuated, which shows the promise of the fabricated fins in robotic fish applications.

The remainder of the paper is organized as follows. The fabrication process for MDOF IPMC actuators is presented in Section 2. In Section 3 we investigate the change of stiffness and swellability of Nafion films induced by the ion-exchange process. The performance of fabricated artificial pectoral fins is characterized in Section 4. Finally, concluding remarks are provided in Section 5.

2. Fabrication process

In this section, we outline the overall fabrication flow first and then discuss the individual steps in more details. Fabrication of an artificial pectoral fin is taken as an example. As illustrated in Fig. 1, the major process steps include:

(a) Create an aluminum mask on Nafion with e-beam deposition, which covers the intended IPMC regions.
(b) Etch Nafion with argon and oxygen plasmas to thin down the passive regions.
(c) Remove the aluminum mask and place the sample in platinum salt solution to perform ion-exchange. This will stiffen the sample and make the following steps feasible.
(d) Pattern with photoresist (PR), where the targeted IPMC regions are exposed while the passive regions are protected.
(e) Perform the second ion-exchange and reduction to form platinum electrodes in active regions. To further improve the conductivity of the electrodes, 100 nm gold is sputtered on the sample surface.
(f) Remove PR and lift off the gold on the passive areas. Soften the passive regions with HCl treatment (to undo the effect of step (c)).
(g) Cut the sample into a desired shape.

2.1. Aluminum mask deposition

Since plasma will be used to selectively thin down the passive areas of the Nafion film, the first step is to make an aluminum mask to protect the active areas from being etched. Two shadow masks made of transparency films are used to cover both sides of the Nafion film, in such a way that the passive areas are covered and the active areas are exposed. The sample is then put into an e-beam deposition system, where aluminum can be deposited at room temperature. Aluminum films of 200 nm thick are deposited on both sides of the Nafion film. When the transparency masks are removed, the aluminum masks stay on the active regions and the sample is ready for plasma etching.

2.2. Plasma etching

Plasma treatment has been used for roughening the Nafion surface to increase the capacitance of IPMC [15]. In this paper, we use plasma to thin down the passive areas in the MDOF IPMC actuator. The plasma etching system used in this research is Plasmaquest Model 357. Experiments have been conducted to study the etching rates with different recipes of gas sources. The etching rates with different recipes are shown in Table 1.

It can be seen that the combination of oxygen and argon plasmas can achieve a higher etching rate than using the oxygen plasma alone. The oxygen plasma performs chemical etching, which can oxidize the polymer and break Nafion into small molecules. The

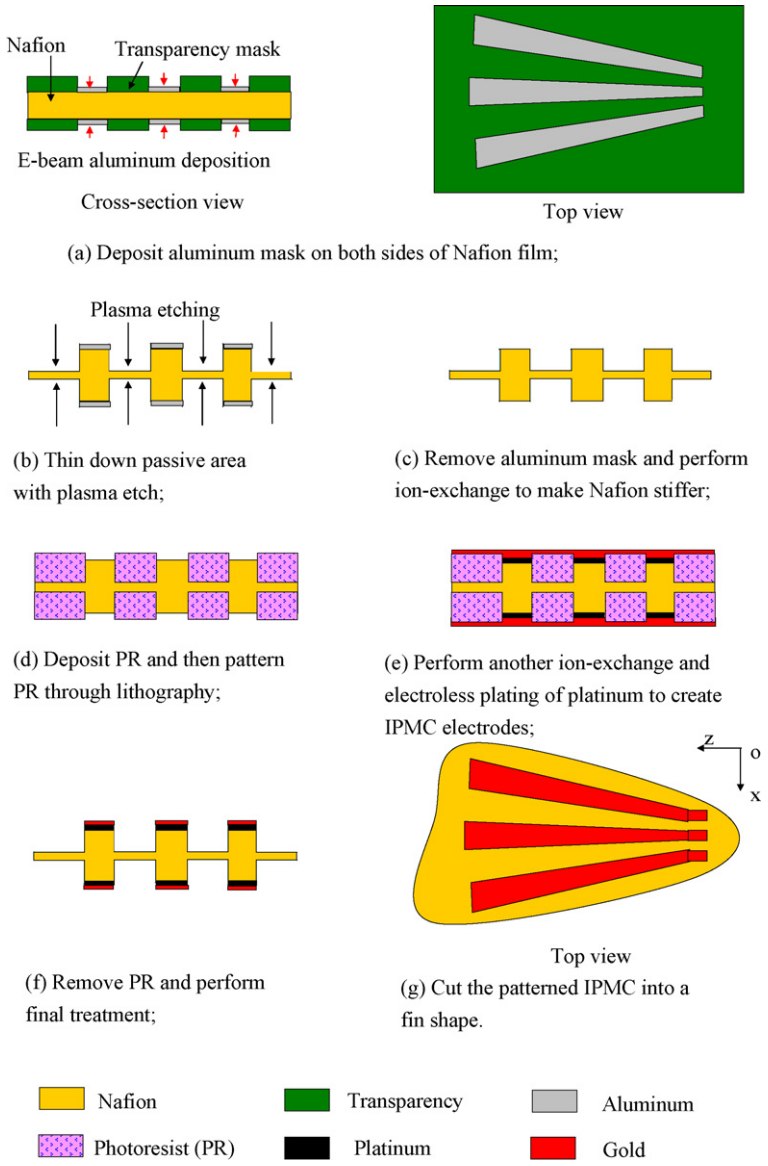

Fig. 1. The process flow for monolithic fabrication of an MDOF IPMC actuator.

higher oxygen flow rate, the higher etching rate but also the higher temperature on the Nafion film. We have found that too strong oxygen plasma will damage the film because of overheating. The argon plasma performs physical etching with high-speed, heavy argon ions. It can remove the small molecules created by the oxygen plasma and roughen the Nafion surface, which creates larger contact area for the oxygen plasma and thus accelerates the chemical etching. The combination of oxygen and argon plasmas can achieve a high etching rate with a low resulting temperature, which is critical to maintaining the original properties of Nafion. In this paper, the recipe *R3* is adopted.

After several hours of plasma etching, the passive areas are thinned down to the desired value. Then the sample is boiled in 2N hydrochloride acid solution at 90 ° C for 30 min to remove the aluminum mask and to remove impurities and ions in Nafion. After that, the membrane is further boiled in deionized (DI) water for 30 min to remove acid. Fig. 2 shows the Scanning Electron Microscope (SEM) picture of a selectively etched Nafion sample, where the thinnest region is 48 μm (down from the original 225 μm). The etched sidewall is almost vertical (the angle is 88°). To roughen the active areas, the sample is treated with plasma for 5 min. This roughening process can enlarge the metal–polymer contact areas, which enhances the actuation performance of IPMC [15].

Table 1
Plasma etching with different recipes.

No.	Ar (sccm)	O_2 (sccm)	RF power (W)	Microwave power (W)	Etching rate (μm/min)
R1	20	30	70	300	0.28
R2	0	50	70	300	0.22
R3	50	30	70	300	0.51

2.3. Stiffening treatment

It is difficult to perform lithography on a pure Nafion film because Nafion swells in the developer, which usually contains water and organic solvent, and the swelling force can easily destroy the photoresist pattern. To address this challenge, we perform an ion-exchange process to impregnate Nafion with large platinum complex ions ($Pt(NH_3)_4^{2+}$). Usually, this ion-exchange process is used to absorb platinum complex ions for electroless platinum plating [30]. However, we have discovered that, after the ion-exchange, the Nafion film becomes stiffer and virtually non-swellable in water

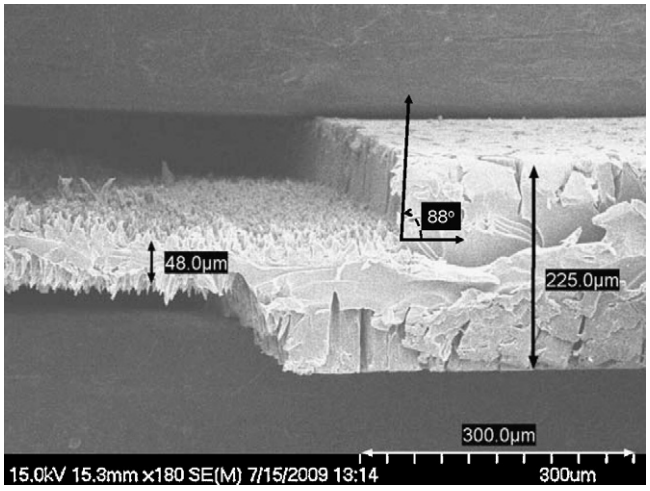

Fig. 2. SEM picture of a plasma-etched Nafion film.

or acetone, which makes lithography and the subsequent patterned electroless plating possible.

To perform ion-exchange, 25 ml of aqueous solution of tetraammine-platinum chloride $[Pt(NH_3)_4]Cl_2$ (2 mg Pt/ml) is prepared with 1 ml of ammonium hydroxide solution (5%) to neutralize. The sample is immersed into the solution at room temperature for 1 day. The impact of stiffening treatment will be studied in detail in Section 3.

2.4. Patterning of Nafion surface

AZ 9260 positive photoresist is selected to create thick PR patterns to protect the passive areas of the actuator from electroless platinum plating. We spin-coat PR at 1000 rpm to get 17 μm thick film and then bake it in oven at 90° C for 2 h. Since the Nafion film alone is not rigid enough for spin-coating and it is easy to deform when baked in oven, an aluminum frame is used to support and fix the Nafion film (25 mm × 25 mm), as shown in Fig. 3. UV light with power density of 20 mW/cm^2 is used to expose the sample with the pattern mask for 105 s. After the sample is exposed, the PR is developed with AZ 400K developer.

2.5. Electroless platinum plating and gold sputtering

The electroless platinum plating process is used to create thick platinum electrodes on the active areas, which results in strong bonding between the metal and the polymer. Three steps are taken for this process. First, another ion-exchange is performed to absorb more platinum complex ions. Second, the sample is put into a bath with DI water at 40 °C. Third, we add 1 ml of sodium boronhydride solution (5 wt% $NaBH_4$) into the bath every 10 min and raise the bath temperature up to 60 ° C gradually. After 30 min of reduction, about 10 μm thick platinum electrodes will grow on the surface of the active areas. To further improve the electrode conductivity, 100 nm thick gold is sputtered on both sides of the sample. The surface resistance can be reduced by half with this gold-sputtering step. Since PR patterns are still on the surface, the passive areas are protected. When the PR is removed with acetone, the gold on the passive areas will be lifted off.

Note that the electroless plating process results in dendritic structures for the electrode-polymer interface [30,31]. While such structures promote electrode-polymer bonding and provide large interfacial area for enhanced actuation performance, they may have implications in the ultimate feature size for the patterned IPMC devices that are fabricated with the proposed method. A related issue in microfabrication is that the reducing agent may "creep" into the boundary of PR-protected area and plate some metal there. These questions need to be explored when one is interested in fabricating devices at the micro scale.

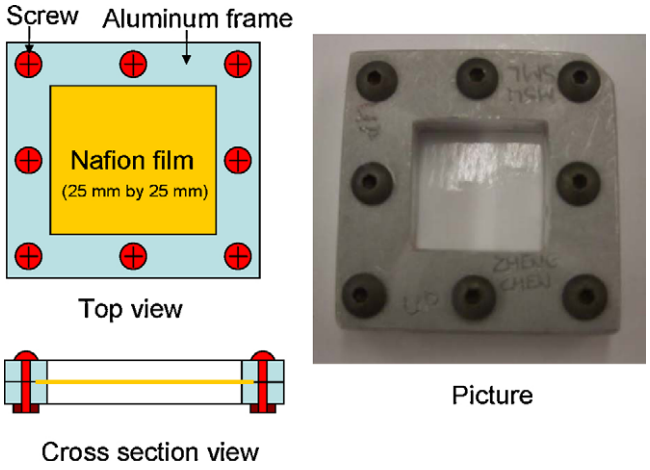

Fig. 3. Nafion film fixed by an aluminum frame.

2.6. Final membrane treatment

After electroless plating, the Pt complex ions in active regions are reduced to platinum metal. But the Pt complex ions in the passive regions are still there, which makes the passive regions stiff. To facilitate 3-D deformation, we need to undo the effect of step (c) to replace the Pt complex ions with H^+. This can be achieved by simply boiling the sample in 2N hydrochloride (HCl) acid [14]. After the sample becomes flexible, it is put into sodium or lithium ion solution (1N) for 1 day to exchange H^+ with Na^+ or Li^+ ions, to enhance actuation of IPMCs.

A fabricated prototype of patterned IPMC membrane is shown in Fig. 4.

3. Impact of stiffening treatment

Stiffening treatment is an important step in fabrication of MDOF IPMC actuators. In this section, we study the impact of the ion-exchange process on the stiffness and swellability of Nafion films, and its implication in lithography and the overall fabrication process.

3.1. Stiffness change

The experimental setup for the stiffness measurement is shown in Fig. 5. The film is fixed at one end by a clamp. A load cell (GS0-10, Transducer Techniques) is mounted on a moving stage (U-SVRB-4, Olympus), which can be manipulated by hand to generate smooth horizontal motion. When the stage is moved, the load cell pushes the Nafion film to bend, and the restoring force at the tip of the film is measured. A laser displacement sensor (OADM 20I6441/S14F, Baumer Electric) is used to measure the corresponding tip displacement. The resolution of the laser sensor is 20 μm and the resolution of the load cell is 0.05 mN. The setup is placed on an anti-vibration table (LW3048B-OPT, Newport). A dSPACE system (DS1104, dSPACE) is used for data acquisition. The spring constant of the Nafion film is calculated as

$$k = \frac{F}{d}, \tag{1}$$

where F and d are the tip force and the tip displacement, respectively.

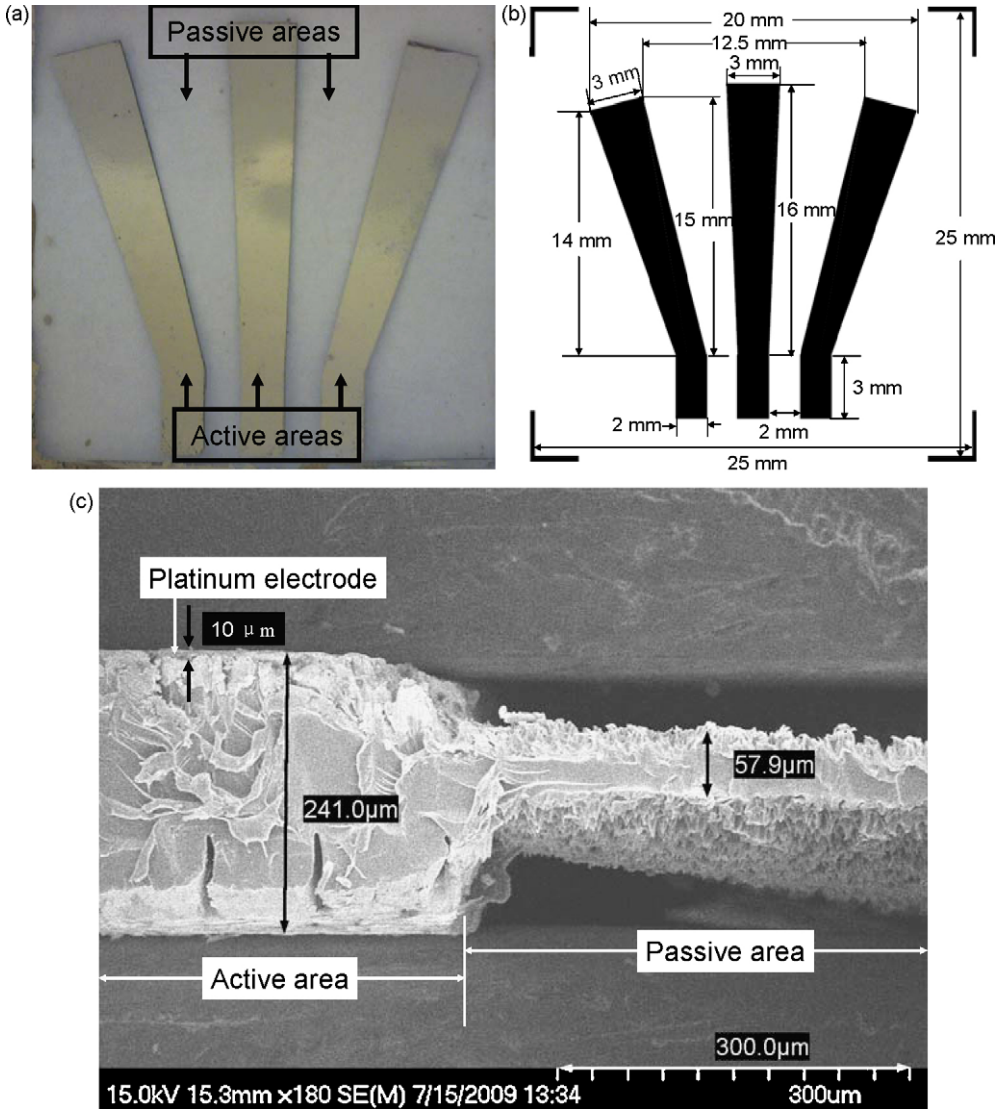

Fig. 4. Patterned IPMC membrane: (a) Top view picture, (b) planar dimensions of the membrane and (c) SEM picture of the cross section.

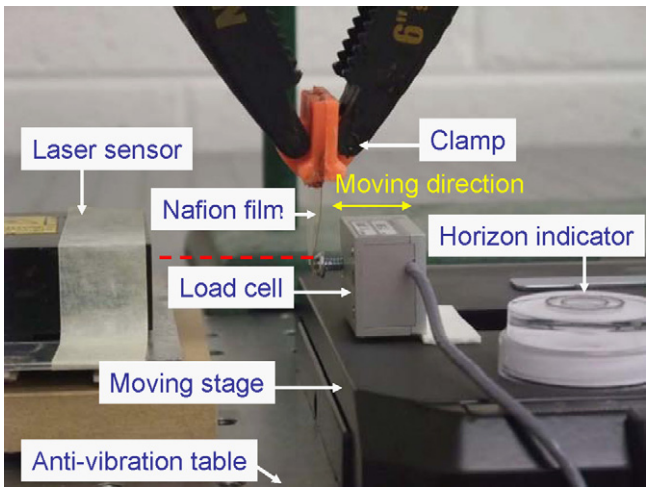

Fig. 5. Experimental setup for measuring the stiffness of a Nafion film.

We have measured the stiffness of Nafion-117 (183 μm) and Nafion-1110 (240 μm) before and after the ion-exchange process. The ion-exchanged Nafion films are dried in air before the experiments. Fig. 6 shows the force and displacement data for each case, together with the results using linear fitting. The spring constant of the cantilever film is

$$k = \frac{YWT^3}{4L^3}, \tag{2}$$

where Y, W, L, and T are the Young's modulus, width, length, and thickness of the Nafion film, respectively. Based on the measured spring constant and dimension parameters, we can calculate the Young's modulus. Table 2 shows the spring constant, dimensions,

Table 2
Spring constant, dimensions, and Young's moduli of the Nafion films in stiffness testing. The ion-exchanged films are identified with an asterisk.

	k (N/m)	W (mm)	L (mm)	T (μm)	Y (MPa)
Nafion-117	1.7 ± 0.2	26 ± 0.1	20 ± 0.1	183 ± 1	355 ± 41
Nafion-117*	6.1 ± 0.4	26 ± 0.1	19 ± 0.1	183 ± 1	1050 ± 68
Nafion-N1110	4.6 ± 0.4	25 ± 0.1	20 ± 0.1	254 ± 1	359 ± 31
Nafion-N1110*	10.2 ± 0.9	25 ± 0.1	21 ± 0.1	254 ± 1	926 ± 69

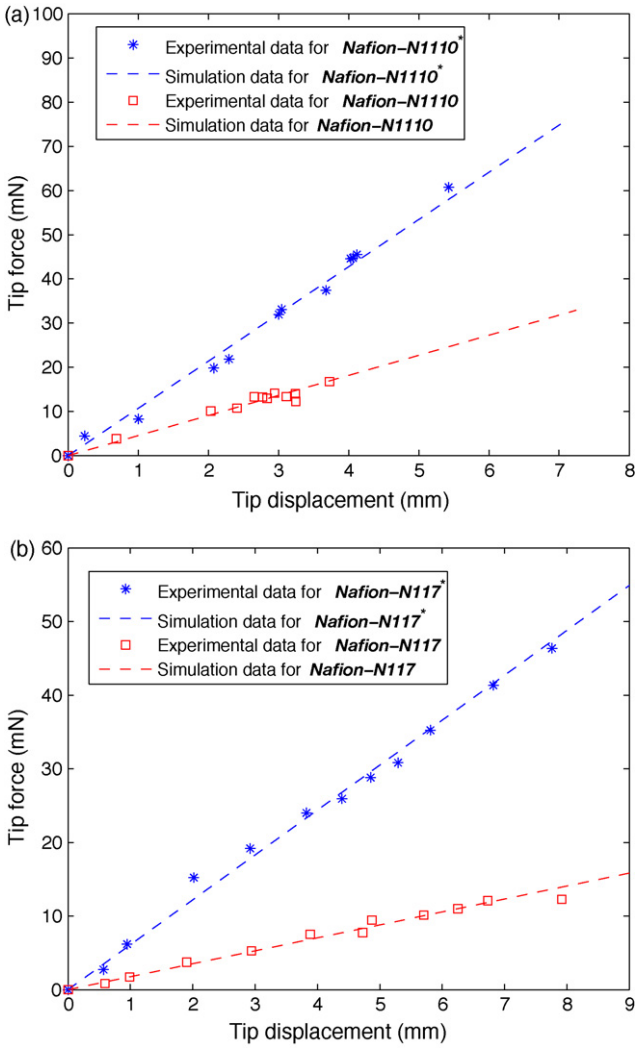

Fig. 6. Results of stiffness measurement: (a) Nafion-N1110 and (b) Nafion-117.

and Young's moduli of the Nafion films. It can be seen that the stiffness of an ion-exchanged Nafion film increases by about 2–3 times, compared to that of pure Nafion.

3.2. Swelling capacity change

We have further investigated the swelling capacity of Nafion before and after the ion-exchange step. Here the swelling capacity is characterized by the change of surface area after a dry sample is soaked in water or acetone. Four samples as listed in Table 3, cut in the rectangular shape, have been tested. A caliper with a resolution of 0.1 mm is used to measure the length L and the width W of the sample, from which the area is determined as LW. Measurements are taken in the following steps. First, the surface areas of the samples in the dry condition are measured.

Table 3
Surface area changes of Nafion films in water and acetone. The ion-exchanged films are identified with an asterisk.

	With water	With acetone
Nafion-117	+19.1%	+59.4%
Nafion-117*	+0.7%	+0.8%
Nafion-N1110	+20.1%	+55.9%
Nafion-N1110*	+1.2%	+1.6%

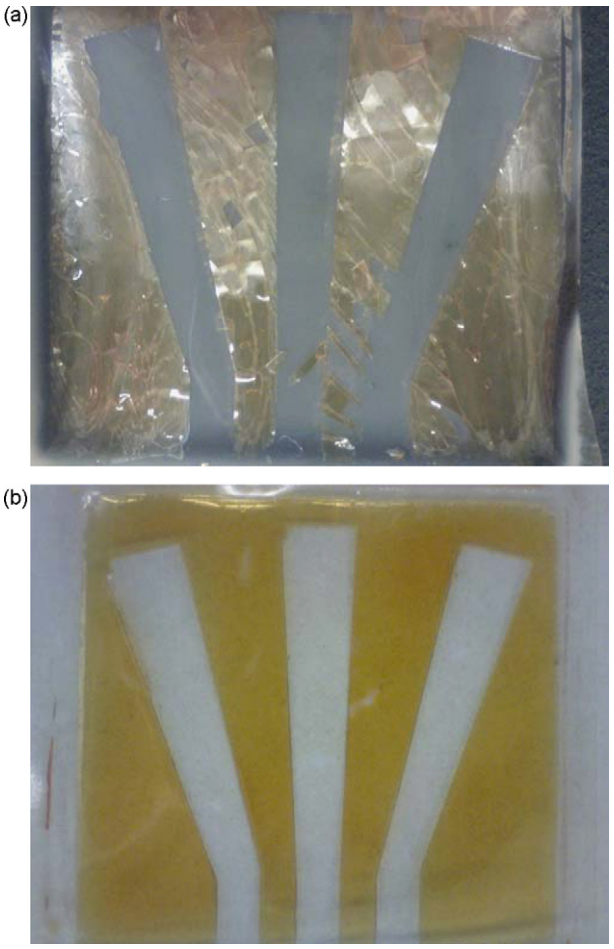

Fig. 7. Lithography results: (a) with pure Nafion and (b) with ion-exchanged Nafion.

Second, the samples are immersed in water for 5 min and then taken out for surface area measurement. Third, the samples are dried with paper towel and in air before being immersed in acetone. After 5 min, the samples are taken out of acetone and their surface areas are measured again. Table 3 shows the percentages of surface area change comparing to the original size, for the four samples, after being soaked in water and in acetone, respectively.

It can be seen that while pure Nafion can expand by about 20% and 60% when soaked in water and in acetone, respec-

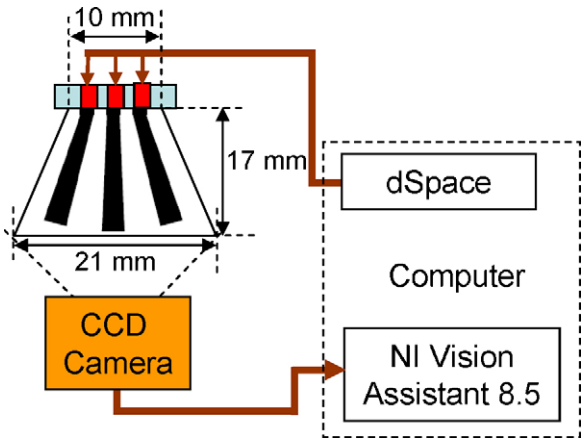

Fig. 8. Experimental setup for characterizing MDOF IPMC actuators.

tively, ion-exchanged Nafion experiences only 1–2% expansion under the same conditions. In other words, ion-exchanged Nafion has very low swellability in solvents, which is important in lithography-based patterning of the film. One possible reason for the significantly reduced swelling capacity is that the film becomes stiffer and the swelling force is unable to enlarge the volume of the film. But the precise explanation of the phenomenon requires further study.

3.3. Impact of ion-exchange on lithography

The impact of ion-exchange process on lithography has been investigated. First, we performed lithography on pure Nafion. When the sample was put into the developer, the film swelled and the PR patterns were destroyed by the swelling force, as shown in Fig. 7(a). Then we performed lithography on ion-exchanged Nafion. The patterning result was sharp, as shown in

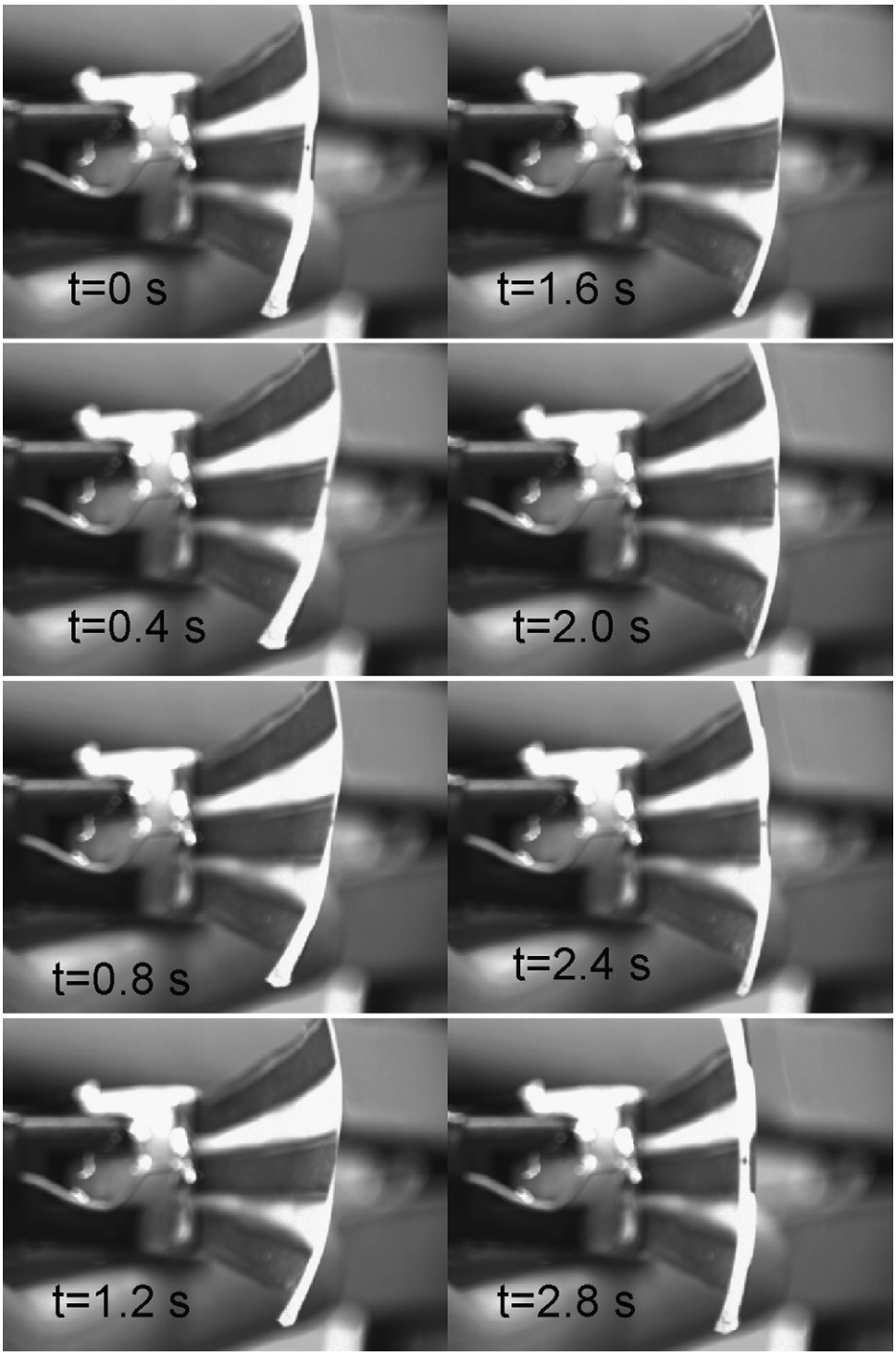

Fig. 9. Snapshots of an actuated MDOF IPMC actuator, demonstrating the twisting motion.

Fig. 7(b). It thus has demonstrated that the lithography of Nafion can be dramatically improved by the stiffening treatment using ion-exchange.

4. Characterization of fabricated artificial fins

4.1. Characterization method

We have characterized the performance of fabricated MDOF IPMC actuators on producing sophisticated shape change. To capture the deformation, one may use multiple laser sensors to detect the bending displacement of active areas [25]. However, when the actuator generates large, complex deformation, some laser sensors can lose measurements. This approach is also expensive. Another approach is to use a CCD camera to capture the video of the actuator movement and then use image processing to extract the actuator movement [32].

The experimental setup we use to characterize MDOF IPMC actuators is shown in Fig. 8. The fabricated IPMC membrane is cut into a pectoral fin shape and its base is fixed by a multi-electrode clamp. The dimensions of the pectoral fin is shown in Fig. 8. To minimize the contact resistance, gold foils (0.1 mm thick) are used to make the contact electrodes. A CCD camera (Grasshopper, Point Grey Research) is oriented toward the edge of the fin. Sinusoid voltage inputs of the same amplitude and frequency but different phases are generated by the dSPACE system and applied to individual IPMC regions. The tip bending displacements of active areas are detected using the image edge detector (Vision Assistant 8.5, National Instruments).

4.2. Demonstration of twisting and cupping

Actuation experiments are first conducted in air. The phase differences between the actuation signals applied to the three IPMC regions could be arbitrary. Since the goal here is to demonstrate sophisticated deformation and not to optimize the control input, we have restricted ourselves to the following particular class of phase patterns: the top IPMC leads the middle IPMC in phase by ϕ, while the bottom IPMC lags the middle IPMC in phase by ϕ. For such a phase pattern, we call it phase ϕ in short.

With all three IPMCs receiving inputs of the same phase (i.e., 0° phase), the fin generates bending. As this is not surprising (a single IPMC produces bending), we will not present the detailed results on bending here. An example of twisting is shown in Fig. 9, where the artificial fin has the same Nafion thickness, 85 μm, in the active and passive areas. The voltages applied are sinusoidal signals with amplitude 3.0 V, frequency 0.3 Hz, and phase 90°. The actuator clearly demonstrates a twisting motion. In order to quantify the twisting deformation, we define the twisting angle θ, which is formed by the line connecting the tips of top and bottom IPMCs with the vertical line m–n, as illustrated in Fig. 10(a). Note that the tip displacements d_1, d_2, d_3 of the IPMC regions are extracted from the video. Fig. 10(b) shows the time trajectories of the displacements

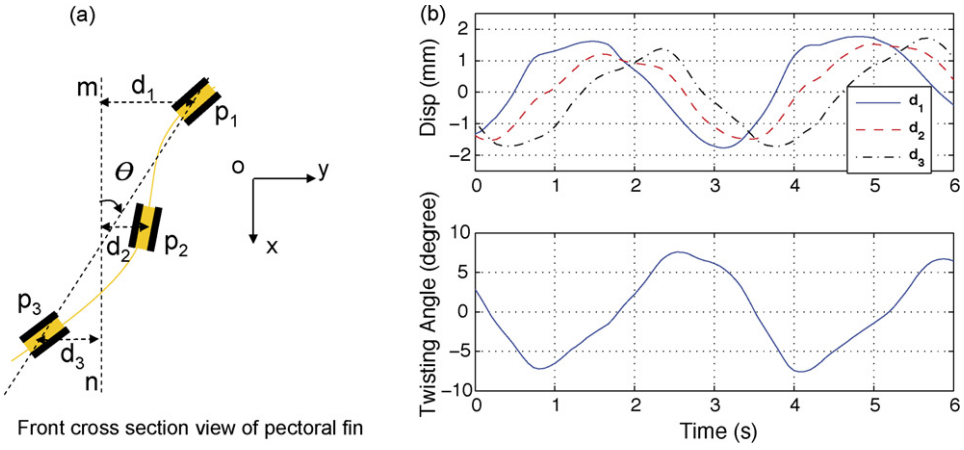

Fig. 10. (a) Definitions of the tip displacements and the twisting angle and (b) trajectories of the tip displacements and the twisting angle corresponding to the voltage inputs as in Fig. 9.

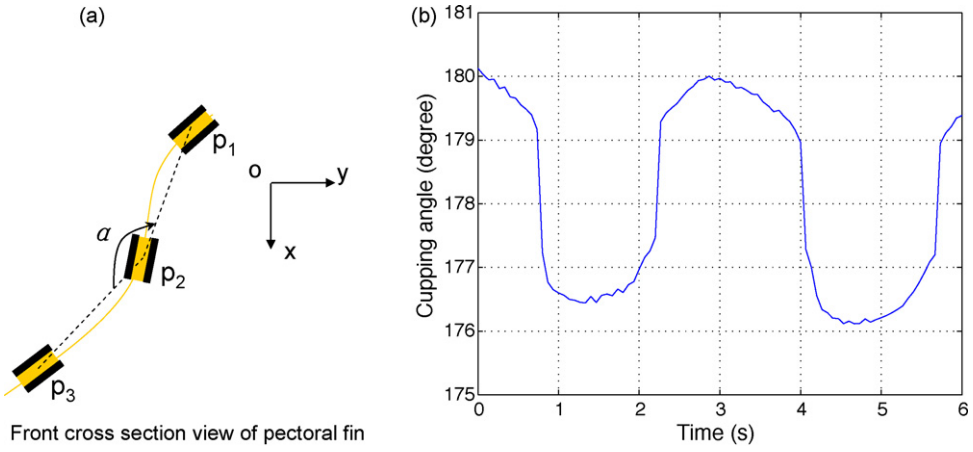

Fig. 11. (a) Definition of the cupping angle and (b) the trajectory of the cupping angle for a sample with 85 μ m thickness in both active and passive areas (voltages: 3 V, 0.3 Hz, 180°).

and the corresponding twisting angle. The twisting angle achieved is 16° peak-to-peak, showing promise in robotic fish applications.

We have also verified the actuator's capability to generate the cupping motion. Fig. 11(a) illustrates the definition of the cupping angle α, formed by the two lines connecting the tip of the middle IPMC to the tips of the top and bottom IPMCs. Fig. 11(b) shows the trajectory of the cupping angle for the same sample mentioned above, where the actuation voltages have amplitude 3.0 V, frequency 0.3 Hz, and phase 180°.

4.3. Impact of the thickness in passive and active areas

To study the effects of thicknesses in active areas and passive areas on the actuation performance, we have fabricated 5 samples with different thicknesses in active areas and passive areas. Table 4 shows the thicknesses of the MDOF IPMC actuators. All actuators have the same planar dimensions as specify in Fig. 4(b). To compare the actuation performance of actuators with different thicknesses in the active areas, we have fabricated three samples (*S1*, *S2*, *S5*), where each sample has the same thickness in its active and passive areas. They are fabricated from Nafion-1110, Nafion-117, and Nafion-1135, respectively. To study the effects of different thickness in passive areas, we have fabricated three samples (*S2*, *S3*, *S4*) with the same thickness in the active areas (170 μm) but different thicknesses in the passive areas. The thickness in active areas refers to that of an original Nafion film based on which the sample is fabricated, and its value is provided by the manufacturer. The thickness in passive areas is controlled through the plasma etch time t_e, and its value is obtained by subtracting $t_e v_e$ from the original Nafion thickness, where v_e denotes the calibrated etch rate (μm/min).

Table 4
Thicknesses of MDOF IPMC actuators.

	Thickness in active area (μm)	Thickness in passive area (μm)
S1	240	240
S2	170	170
S3	170	120
S4	170	60
S5	85	85

The twisting angles generated by different samples with 0.3 Hz, 3 V and 90° phase voltage signals are shown in Fig. 12. From Fig. 12(a), for samples with uniform thickness, the thinner the sample is, the larger the deformation. This can be explained by that, under the same voltage, a thinner sample

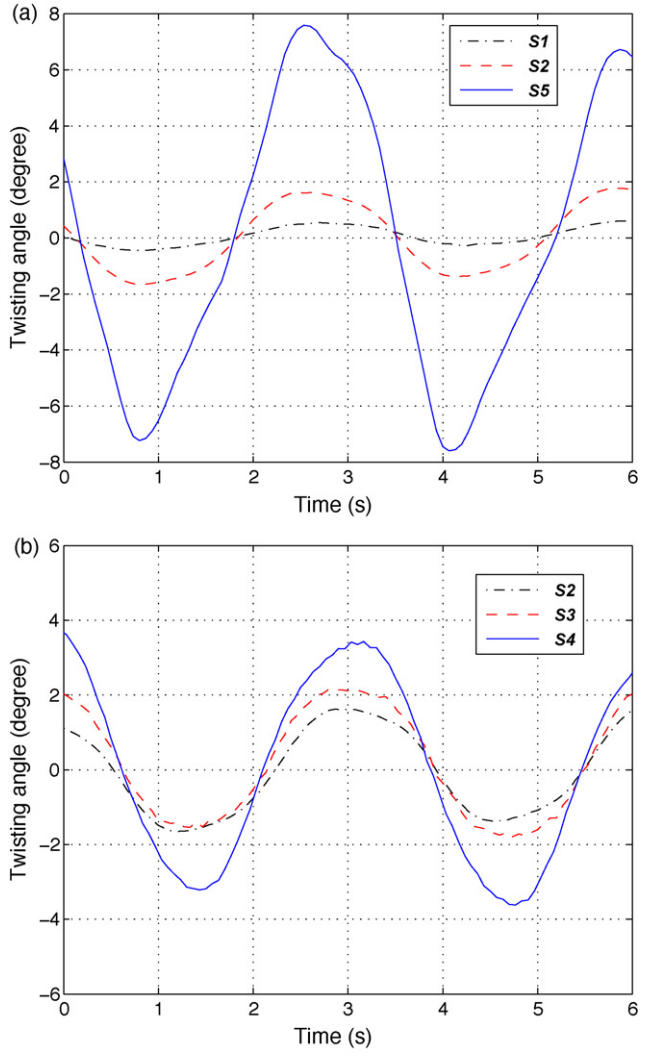

Fig. 12. Twisting angles generated by different samples with 0.3 Hz, 3 V and 90° phase sinusoid voltage signals. (a) MDOF IPMC actuators with different thickness in both active areas and passive areas. (b) MDOF IPMC actuators with the same thickness in active areas (170 μm) but different thicknesses in passive areas.

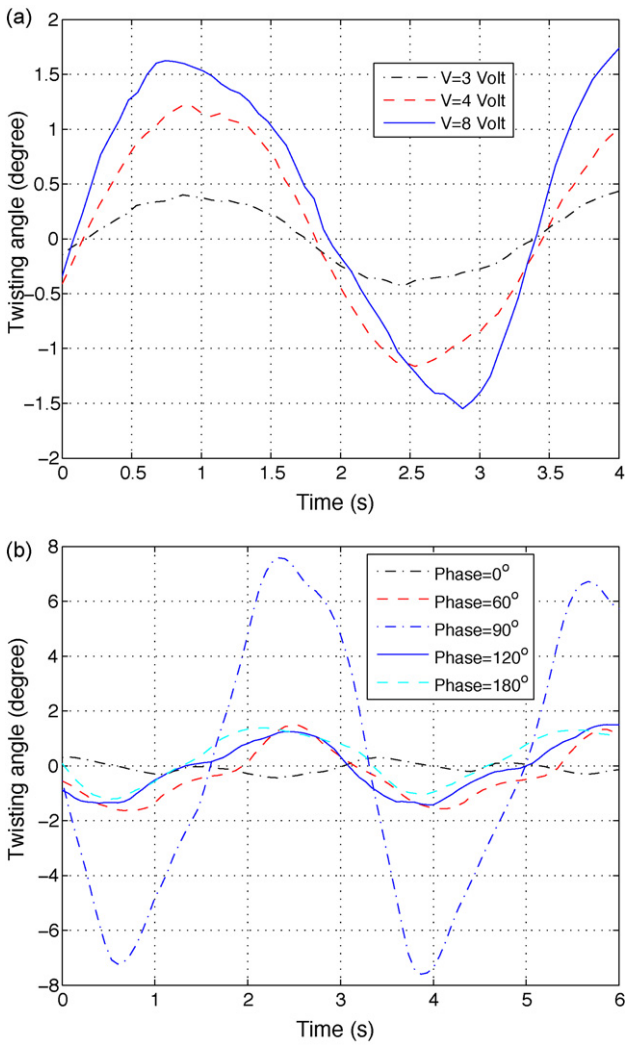

Fig. 13. (a) *S1* actuated by voltage signals with different amplitudes but the same frequency (0.3 Hz) and phase (90°). (b) *S5* actuated by voltage signals with the same amplitude (3 V) and frequency (0.3 Hz) but different phases.

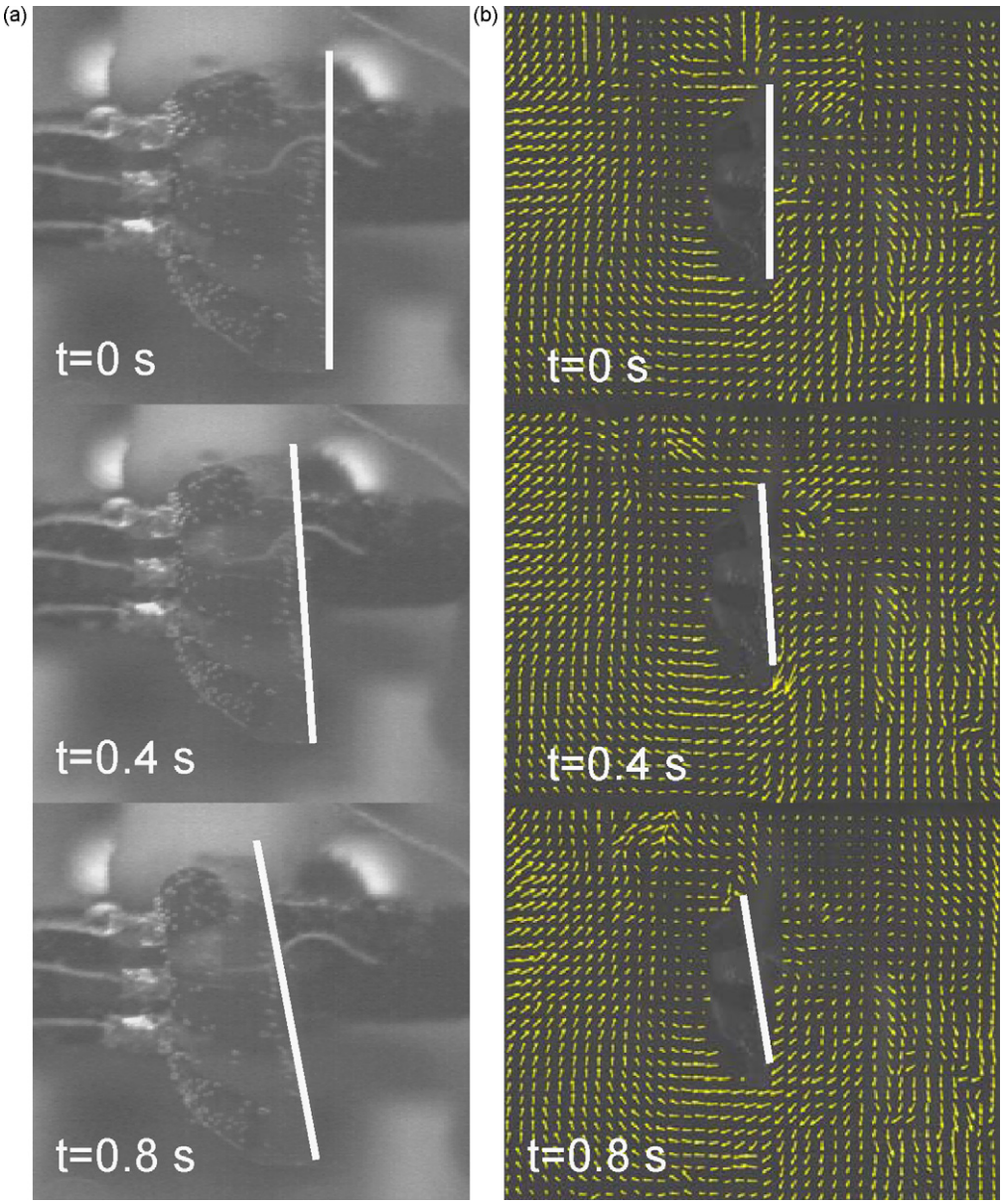

Fig. 14. DPIV study of MDOF IPMC actuator operating in water. (a) Actuation of the actuator in water (the edge of the actuator is highlighted). (b) Velocity field of the fluid.

experiences higher electrical field, and that a thinner sample is more compliant. From Fig. 12(b), it can be seen that for samples with the same thickness in active areas, with thinner passive regions, the deformation gets larger under the same voltage inputs. This has thus provided supporting evidence for our approach of modulating mechanical stiffness through plasma etching.

4.4. Impact of actuation signals

We have further experimented with actuation signals with different phases and amplitudes. Table 5 shows all the actuation signals we have used in the experiments. We have selected *S1* and *S5* as the test samples. All the signals have the same frequency 0.3 Hz. To study the effects of phase on the actuation performance, the voltage signals from *Control #1* to *Control #5* have the same amplitude (3 V) but different phases. To understand the performance of an MDOF IPMC actuator under different voltage levels, the voltage signals from *Control #5* to *Control #7* have the same phase (90°) but different amplitudes.

Fig. 13(a) shows the twisting angle of *S1* actuated under different voltage levels but with the same phase and frequency. While as expected, the higher the voltage, the larger the twisting, the gain in deformation does not appear to be linearly growing with the voltage level. Such nonlinearities will be examined in our future work. Fig. 13(b) shows the twisting angle of *S5* actuated by the same voltage amplitude but different phases. From the figure, 90° appears to be the best phase to generate the twisting motion, the reason of which will be explored in our future modeling work.

Table 5
Actuation signals.

	Frequency (Hz)	Amplitude (V)	Phase (°)
Control #1	0.3	3	180
Control #2	0.3	3	120
Control #3	0.3	3	60
Control #4	0.3	3	0
Control #5	0.3	3	90
Control #6	0.3	4	90
Control #7	0.3	8	90

4.5. DPIV study on MDOF IPMC actuation in water

In the interest of robotic fish applications, we have also conducted preliminary study of underwater operation of the MDOF IPMC actuators. Digital Particle Image Velocimetry (DPIV) system is used to observe fluid motion generated by the actuator. In a DPIV system, small particles are dispersed in a fluid and a laser sheet is created in the fluid to illuminate the particles. Processing of images taken in quick successions can reveal the movement of particles and provide information about the flow fluid. We have tested sample *S5* in water, by applying voltage signals (4 V, 0.3 Hz, and 90° phase) to the actuator. Fig. 14(a) shows the snapshots of the MDOF IPMC actuation in water. Fig. 14(b) shows the velocity field of the water around the actuator. It demonstrates that the MDOF IPMC actuator can make 3-D deformation in water and can generate some interesting flow patterns around it. The connections between the flow patterns and the actuator deformations are a subject of future investigation.

5. Conclusions and future work

In this paper we have presented a new process flow for monolithic, batch-fabrication of MDOF IPMC actuators. The methodology effectively incorporates standard techniques for IPMC fabrication and lithography-based micromachining processes. The actuator consists of multiple IPMC islands coupled through a passive membrane. The size and shape of each IPMC island are defined through photolithography and thus the approach is scalable. A key innovation in the developed process is to stiffen the Nafion film through an ion-exchange step, which virtually eliminates swelling in solvents and enables successful patterning. Tailoring the thickness and thus the rigidity of the passive area is another novel aspect of the proposed fabrication method. The fabrication method has been applied to manufacture prototypes of biomimetic fins, with demonstrated capability of producing complex deformation modes such as twisting and cupping.

The prototypes fabricated in this work have dimensions of centimeters because of our interest in biomimetic actuation for robotic fish applications. The developed fabrication process can be extended easily to produce microscale devices since it is based on MEMS processes. As discussed in Section 2.5, however, the electroless plating process may impose a limit on the smallest feature size that can be achieved, and it will be of interest to characterize this limit and examine how to reduce it by modulating the electroless plating process. We also note that, while commercially available Nafion films have been used as the base material in our work, the approach can be easily extended to Nafion membranes obtained through casting, and to other types of ion-exchange membranes (e.g., Flemion).

Future work includes understanding and modeling of MDOF IPMC actuators, by extending the authors' prior work [33] on modeling of IPMC beams. The interactions between the active IPMC regions and the passive regions will be a focus of study. We will also investigate systematically the hydrodynamics in underwater operation of such MDOF IPMC actuators, using a combination of analytical modeling, computational fluid dynamics (CFD) modeling, and DPIV studies, and explore the use of these actuators in biomimetic robotic fish.

Acknowledgments

This research was supported in part by an ONR grant (N000140810640, program manager Dr. T. McKenna) and an NSF CAREER grant (ECCS 0547131). We would like to thank Dr. Baokang Bi, Karl Dersch, Dr. Hoyin Chan, and Yixing Wang, for providing help on our fabrication work.

References

[1] M. Shahinpoor, K. Kim, Ionic polymer–metal composites: I. Fundamentals, Smart Materials and Structures 10 (2001) 819–833.
[2] Y. Bar-Cohen, Electric flex, IEEE Spectrum 41 (6) (2004) 29–33.
[3] K.J. Kim, M. Shahinpoor, Ionic polymer–metal composites: II. Manufacturing techniques, Smart Materials and Structures 12 (2003) 65–79.
[4] S. Tadokoro, S. Yamagami, M. Ozawa, Soft micromanipulation device with multiple degrees of freedom consisting of high polymer gel actuators, in: Proceedings of IEEE International Conference on Micro Electro Mechanical Systems, 1999, pp. 37–42.
[5] S. Guo, T. Fukuda, K. Asaka, A new type of fish-like underwater micro-robot, IEEE/ASME Transactions on Mechatronics 8 (1) (2003) 136–141.
[6] B. Kim, J. Ryu, Y. Jeong, Y. Tak, B. Kim, J.-O. Park, A ciliary based 8-legged walking micro robot using cast IPMC actuators, in: Proceedings of IEEE International Conference on Robots and Automation, 2003, pp. 2940–2945.
[7] M. Shahinpoor, K. Kim, Ionic polymer–metal composites: IV. Industrial and medical applications, Smart Materials and Structures 14 (2005) 197–214.
[8] M. Yamakita, N. Kamamichi, T. Kozuki, K. Asaka, Z. Luo, Control of biped walking robot with IPMC linear actuator, in: Proceedings of the IEEE/ASME International Conference on Advanced Intelligent Mechatronics, Monterey, CA, 2005, pp. 48–53.
[9] X. Tan, D. Kim, N. Usher, D. Laboy, J. Jackson, A. Kapetanovic, J. Ra-pai, B. Sabadus, X. Zhou, An autonomous robotic fish for mobile sensing, in: Proceedings of the IEEE/RSJ International Conference on Intelligent Robots and Systems, Beijing, China, 2006, pp. 5424–5429.
[10] Z. Chen, Y. Shen, N. Xi, X. Tan, Integrated sensing for ionic polymer–metal composite actuators using PVDF thin films, Smart Materials and Structures 16 (2) (2007) S262–S271.
[11] Z. Chen, S. Sharata, X. Tan, Modeling of biomimetic robotic fish propelled by an ionic polymer metal composite caudal fin, IEEE/ASME Transactions on Mechatronics, in press, doi:10.1109/TMECH.2009.2027812.
[12] K. Oguro, Y. Kawami, H. Takenaka, Bending of an ion-conducting polymer film–electrode composite by an electric stimulus at low voltage, Journal of Micromachine Society 5 (1992) 27–30.
[13] J. J. Pak, J. Kim, S. W. Oh, J. H. Son, S. H. Cho, S.-K. Lee, J.-Y. Park, B. Kim, Fabrication of ionic-polymer–metal-composite (IPMC) micropump using a commercial Nafion, in: Y. Bar-Cohen (Ed.), Smart Structures and Materials 2004: Electroactive Polymer Actuators and Devices (EAPAD), Proceeding of SPIE, vol. 5385, 2004, pp. 272–280.
[14] K.J. Kim, M. Shinpoor, A novel method of manufacturing three-dimensional ionic polymer–metal composites (IPMCs) biomimetic sensors, actuators, and artificial muscles, Polymer 43 (2002) 797–802.
[15] S.J. Kim, I.T. Lee, Y.H. Kim, Performance enhancement of IPMC actuator by plasma surface treatment, Smart Materials and Structures 16 (1) (2007) N6–N11.
[16] C. Chung, P. Fung, Y. Hong, M. Ju, C. Lin, T. Wu, A novel fabrication of ionic polymer–metal composites (IPMC) actuator with silver nano-powders, Sensors and Actuators B: Chemical 117 (2006) 367–375.
[17] B.J. Akle, M.D. Bennett, D.J. Leo, High-strain ionomeric-ionic liquid electroactive actuators, Sensors and Actuators A 126 (2006) 173–181.
[18] S. Tung, S.R. Witherspoon, L.A. Roe, A. Silano, D.P. Maynard, N. Ferraro, A MEMS-based flexible sensor and actuator system for space inflatable structures, Smart Materials and Structures 10 (6) (2001) 1230–1239.
[19] G.V. Lauder, E.J. Anderson, J. Tangorra, P.G.A. Madden, Fish biorobotics: kinematics and hydrodynamics of self-propulsion, Journal of Experimental Biology 210 (2007) 2767–2780.
[20] S.-W. Yeom, I.-K. Oh, A biomimetic jellyfish robot based on ionic polymer metal composite actuators, Smart Materials and Structures 18 (2009) 085002:1–08500210:08500210.
[21] P. Meissner, B.K.A.F. Riemenschneider, H. Halbritter, S. Jatta, M. Maute, M.C. Amann, Tunable long-wavelength VCSELs using a moveable mirror membrane, in: Proceedings of the 18th Annual Meeting of the IEEE Lasers and Electro-Optics Society, 2005, pp. 324–325.
[22] G.V. Lauder, P.G.A. Madden, Learning from fish: kinematics and experimental hydrodynamics for roboticists, International Journal of Automation and Computing 4 (2006) 325–335.
[23] D. Dogruer, J. Lee, W. Yim, K. Kim, D. Kim, Fluid interaction of segmented ionic polymer–metal composites under water, Smart Materials and Structures 16 (2007) 220–S226.
[24] J.-H. Jeon, I.-K. Oh, J.-H. Han, S.-W. Lee, Development of bio-mimetic patterned IPMC actuators with multiple electrodes, Key Engineering Materials 334–335 (2007) 1005–1008.
[25] J.-H. Jeon, S.-W. Yeom, I.-K. Oh, Fabrication and actuation of ionic polymer metal composites patterned by combining electroplating with electroless plating, Composites Part A: Applied Science and Manufacturing 39 (2008) 588–596.
[26] J.-H. Jeon, I.-K. Oh, Selective growth of platinum electrodes for MDOF IPMC actuators, Thin Solid Films 517 (2009) 5288–5292.
[27] S. Tung, B. Maines, F. Jiang, T. Tsao, Transonic flow separation control by MEMS sensors and actuators, in: Proceedings of 39th AIAA Aerospace Sciences Meeting & Exhibit, Reno, NV, 2001, AIAA Paper 2001–0123.

[28] J.W.L. Zhou, H.-Y.C.A.K.H. To, K.W.C. Lai, W.J. Li, Polymer, MEMS actuators for underwater micromanipulation, IEEE/ASME Transactions on Mechatronics 9 (2) (2004) 334–342.
[29] G.-H. Feng, R.-H. Chen, Improved cost-effective fabrication of arbitrarily shaped IPMC transducers, Journal of Micromechanics and Micro-engineering 015016 (1) (2008) 1–9.
[30] M. Shahinpoor, K.J. Kim, The effect of surface-electrode resistance on the performance of ionic polymer–metal composite (IPMC) artificial muscles, Smart Materials and Structures 9 (2000) 543–551.
[31] S. Nemat-Nasser, Y. Wu, Comparative experimental study of ionic polymer–metal composites with different backbone ionomers and in various cation forms, Journal of Applied Physics 93 (9) (2003) 5255–5267.
[32] G. Del Bufalo, L. Placidi, M. Porfiri, A mixture theory framework for modeling the mechanical actuation of ionic polymer metal composites, Smart Materials and Structures 10 (2008) 0450101–04501014.
[33] Z. Chen, X. Tan, A control-oriented and physics-based model for ionic polymer–metal composite actuators, IEEE/ASME Transactions on Mechatronics 13 (5) (2008) 519–529.

Biographies

Zheng Chen received the BS degree in electrical engineering and the MS degree in control science and engineering from Zhejiang University, Hangzhou, China, in 1999 and 2002, respectively. He received his PhD degree in electrical engineering at Michigan State University (MSU), East Lansing, in 2009. Afterwards, he joined the Department of Mechanical & Aerospace Engineering at the University of Virginia as a research associate. His current research interests include fabrication, modeling and control of electrical-active polymers (EAPs), biomimetic robots, EAP-based smart microsystems, and optimal control using neural networks. Dr. Chen was the recipient of a Summer Dissertation Fellowship in 2005 and a Dissertation Completion Fellowship in 2009, both from MSU Graduate School. He also received an Honorable Mention for the Fitch Beach Outstanding Graduate Research Award from MSU College of Engineering in 2008 and a Valued Reviewer Award from Sensors and Actuator A: Physical in 2009.

Xiaobo Tan received the Bachelor's and Master's degrees in automatic control from Tsinghua University, Beijing, China, in 1995 and 1998, respectively, and the PhD degree in electrical and computer engineering from the University of Maryland, College Park, in 2002. From September 2002 to July 2004, he was a research associate with the Institute for Systems Research at the University of Maryland. Since August 2004, he has been an assistant professor in the Department of Electrical and Computer Engineering and Director of Smart Microsystems Laboratory at Michigan State University. His current research interests include electroactive polymer sensors and actuators, aquatic robotics, modeling and control of smart materials, and adaptive autonomous cyber-physical systems. Dr. Tan is an Associate Editor of Automatica and a member of the IEEE Control Systems Society Conference Editorial Board. He was a Guest Editor of IEEE Control Systems Magazine for its February 2009 issue's special section on modeling and control of hysteresis. He received the NSF CAREER Award in 2006, the 2008 ASME DSCD Best Mechatronics Paper Award, and the Teacher-Scholar Award from Michigan State University in 2010.